

# Experimental report

19/05/2021

**Proposal:** 1-05-14

**Council:** 4/2020

**Title:** Discerning dynamics of wormhole growth at sub-resolution scale using combined Neutron and X-Ray Tomography

**Research area:** Physics

**This proposal is a new proposal**

**Main proposer:** Max COOPER

**Experimental team:** Piotr SZYMCZAK  
Max COOPER

**Local contacts:** Alessandro TENGATTINI

**Samples:** limestone

Instrument	Requested days	Allocated days	From	To
NEXT	3	3	03/09/2020	06/09/2020

## Abstract:

The formation of wormholes during the dissolution of porous media is a multi-scale multi-physics phenomenon, coupling flow and transport at the pore-scale to the evolving geometry of the macro-scale features. The dynamics of macro-scale wormhole formation can be captured with sequential X-Ray tomography (XT) imaging, however time-resolution tradeoffs prevent capture of smaller scale dynamics. A previous experiment using neutron tomography (NT) with heavy-light water contrast captured highly focused fluid flow past the tip region of a wormhole, indicating control control by both large-scale heterogeneities within the matrix and microporosity. Additionally, when the flow field is calculated numerically from one XT image in a time series, the wormhole in the following image tracks one flow path. We request three days of beamtime on the D50T instrument to perform several experiments where a sample is acidized to form a wormhole. The dynamics of macro-scale evolution of the wormhole will be captured with XT at a sufficient resolution, with dissolution paused periodically to perform a flow field experiment with NT to verify if flow fields govern the future wormhole growth.

## Discerning dynamics of wormhole growth at sub-resolution scale using combined Neutron and X-Ray Tomography

Experiment 1-05-14, September 2020

Max Cooper, Silvana Magni, Rishabh Sharma, Tomasz Blach, Andrzej Radlinsky, Piotr Szymczak

Two acidization experiments (PIN43, PIN44) were conducted on cores of Pinczow Limestone to capture dynamics of wormhole growth. These experiments combined X-Ray tomography to capture the macro, geometric growth of the wormhole, with neutron tomography to capture flow paths through the porous regions ahead of the wormhole. This study was motivated by a previous experiment (PIN02, UGA-59) performed on the Neutron and X-Ray Tomograph (NeXT) instrument at ILL. In experiment PIN02 the core was first acidized with HCl diluted in H<sub>2</sub>O under conditions to establish a wormhole in the dominant regime, while being scanned with X-Ray tomography. After the wormhole propagated partially through the core acidization was ceased, the acid and remaining H<sub>2</sub>O were flushed with D<sub>2</sub>O, followed by injection of H<sub>2</sub>O as a neutron contrast agent to image fluid flow. Flow through the sample was highly focused in the wormhole as expected. Interestingly, flow beyond the tip remains similarly focused into the porous region, showing preferential flow paths guided by features smaller than the resolvable X-Ray resolution used to observe geometry changes (Cooper et al., 2019). Subsequent modeling of flow fields using a Darcy-Brinkman solver with time series X-Ray tomography data from the experiment showed that geometry of the wormhole's future path was guided by this flow field. As such, experiments PIN43 and PIN44 sought to demonstrate focused flow predicting future growth of a wormhole experimentally, with a secondary aim to capture high temporal resolution geometry changes.

Experiments PIN43 and PIN44 were performed with the same apparatus as the PIN02 experiment, except a different dissolution cell was used, allowing cores up to 38.3mm in diameter and 12.5cm in length. Instead of acidizing with HCl diluted in H<sub>2</sub>O, the acid was diluted in D<sub>2</sub>O to skip the flushing step. Further, acidization was resumed after flow fields were measured. To enable the entire core geometry to be scanned without moving the z-axis, cores of Pinczow Limestone 38.3mm in diameter and 60mm in length were used. Temporal resolution during dissolution was optimized to enable scanning at 45 micrometer voxel resolution with the duration of the experiment. Dissolution was paused several times throughout the experiments to capture the flow field. To minimize setup time for these portions of the experiment acid was flushed from the inlet lines with an air-filled syringe, followed by priming the lines with H<sub>2</sub>O, which was pushed by the acidic solution. Acquisition times for capturing flow with neutron tomography were determined during the first flow measurement, with flow rate adjusted to minimize scan time yet maintain quality. X-Ray capture was resumed after pumping the inlet line's volume as indicated in pump software to resume the dissolution phase of the experiment. In addition to tomography, pressure difference across the cell was logged every second.

Experiment PIN43 was designed to produce a dominant wormhole with a flow rate of 0.5mL/min. The planned duration of dissolution was 12 hours, with four flow field experiments each lasting ~1 hour. With the chosen parameters, an HCl concentration of 0.1M was determined from previous laboratory experiments. To maximize the number of scans during the formation of a dominant wormhole an 8-minute X-Ray scan time was used. An initial flow experiment was performed prior to acidization to determine if there were any pre-existing flow paths by first saturating the sample with heavy water and light water in the cell inlet line. Neutron and X-Ray tomography was performed with an 8-minute scan time, followed by just X-Ray acquisition once the cell inlet line was full of acid. Further flow field capturing was performed after ~9 hours of dissolution, ~12 hours of dissolution, and ~14.5 hours of dissolution, with breakthrough occurring at ~16 hours. Neutron tomography acquisition time was adjusted after the first interim flow measurement to 4-minutes as the volume of accessible pores was decreased due to wormhole formation. Experiment PIN44 was designed to produce a conical wormhole, with a flow rate of 0.125mL/min. To decrease the time for the instability formation, a small hole ~5mm deep was drilled in the center of the core. This experiment was not intended to reach the breakthrough due to the large length of time required. Instead, the experiment was run from the end of PIN43 until the end of the allotted beamtime. HCl concentration was chosen to be 0.8M. As conical wormholes have been observed to grow more slowly in the flow direction, acquisition time of 20 minutes was chosen as it produces higher quality imagery than faster scans. As in PIN43, an initial flow field was measured, though in this experiment 4-minute scans were taken. Similarly, an intermediate flow field experiment was performed, however, in this experiment only one flow field measurement was performed due to pump failure partially through the experiment. This intermediate flow measurement was conducted after ~9 hours of dissolution. Due to the length of repair time, the total dissolution time for PIN44 was 17 hours.

For PIN43 a dominant wormhole was formed (Fig. 1). Time series X-ray data reveal the wormhole grows at a steady velocity through the bulk of the core, with interspersed times of higher velocity (jumps). Steady velocity periods correspond to plateau regions in the measured differential pressure through the sample (Fig. 2), despite little change in differential pressure. Interestingly, the type of pressure curve in Fig. 2 contrasts with the majority of reported pressure curves in the literature, where pressure drop over time is linear. However, the type of growth captured from tomography and pressure evolution does align with our previous experiments

performed on Pinczow Limestone (PIN02) and some other limestone dissolution experiments in the literature (Bazin 1995, Izgec 2010). The flow portions of the experiment show flow focusing past the tip of the wormhole as resolvable with the X-ray resolution, with dispersion farther into the porous regions. Upon subsequent dissolution future wormhole growth follows the focused path until the dispersion region. Experiment PIN44 formed a conical wormhole (Fig. 3) and is the first conical experiment the group has successfully captured over a long period with full X-Ray tomography, as during the previous conical experiment performed at ILL (PIN01) acquisition was changed to few-angle radiographs after the initial stage. In PIN44 the wormhole initiated similarly to a dominant wormhole, with a thin channel of similar width throughout, propagating through the sample. After quick propagation the wormhole widened into a conical wormhole. After some widening quick jumps again occurred in a similar style to dominant wormhole growth, followed again by widening. This process occurred several times during the experiment.

Preliminary, qualitative, analysis of flow data from PIN43 shows that the flow field in the sub-resolved pore space ahead of the wormhole tip governs the future path of the wormhole to a very high extent. For instance, in Fig. 1C,D, the wormhole after dissolution is resumed closely tracks the focused flow, even following a tortuous path in the flow field. While the main path of the wormhole tracks the flow path, some side branches do occur that are not predicted. Subsequent flow capture shows these side branches to be inactive, as they receive flow but do not focus flow into the surrounding porous matrix.

While the analysis of the flow field using the data acquired in these experiments is still in progress, the geometrical data from PIN43 is being utilized in a manuscript that is currently being written. This manuscript focuses on the reason for the plateau and jump behavior in Pinczow pressure curves. A simple Darcy reactive flow model produces similar dynamics of large tip and pressure drop jumps when less permeable layers are introduced. To determine if the Pinczow samples used in these experiments contain such layers that can be used to explain the pressure curves the variability of porosity along the sample was analyzed from initial tomography prior to acidization. A simple measurement of the sum of grayscale intensities in cross-sections perpendicular to the sample axis is used as a proxy for porosity/permeability, as larger intensities are related to crystalline fossil grains, and thus the larger the sum the larger the grain content and lower the permeability. To ensure that larger intensities are related to grains, multiple thin sections were taken from a sample and compared to tomography, the result of which corresponds to the large intensity/grain hypothesis. Trends of grayscale sums show definite regions with higher grain content and others dominated by a mixture of pores and grains lower than the scanning resolution (microporosity). Tip position over time was then compared to the grayscale sum, which indicates jumps in tip position correspond to regions of packed grains (Fig. 4). In addition to tip position, several other measurements of geometry were also taken, including the number of new branches per time (Fig. 2). The trend of new branches per time shows a large amount of branching while the wormhole is moving through the microporous region, with fewer branches forming while growing through the packed regions. Additionally, the number of branches tends to increase prior to the wormhole entering the packed region. As such, the interpreted reason for large wormhole velocities through the packed region is a feedback of fewer available paths through the packed region, decreasing the number of active branches. A decrease in the amount of active branches then increases local flow velocity as volumetric flow rate is less divided. Consequently, larger flow velocities increase the penetration length for dissolution. Another interpretation from the data is that the pressure curve together with the tip position curve act as a probe, first probing the nature of the rock (e.g., presence of lack of layers, large vugs), and further, the location of features. This opens up a possibility of using wormholing as a testing tool for the assessment of the rock heterogeneity and microlayering.

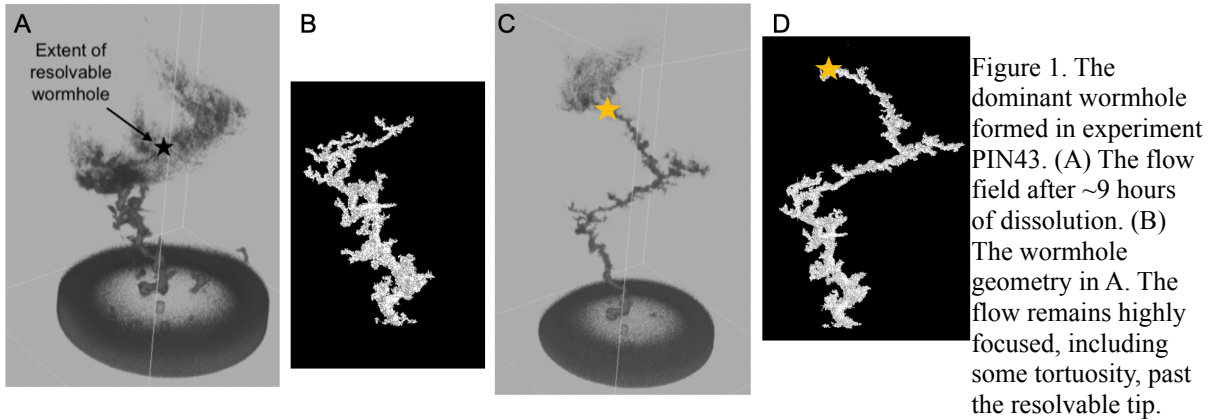
The experiments performed during the beamtime on the NeXT instrument allotted to our group have given data for both the proposed study related to the prediction of future wormhole growth by flow field as captured with neutron tomography, and the separate study related to geometrical growth of wormholes in Pinczow limestone. As mentioned above, a manuscript is currently being prepared related to the secondary purpose of these experiments, including data from other experiments performed by our group at other tomographs. That study is nearly complete regarding analyses, and the writing phase has begun. Further, quantitative work will be done on the flow field portions of the experiment, where the full capabilities of NeXT was used in both the previous experiment at ILL and the two experiments performed in this report.

#### References

- Bazin, B., C. Roque, and M. Bouteca. "A Laboratory Evaluation of Acid Propagation in Relation to Acid Fracturing: Results and Interpretation." *SPE European Formation Damage Conference*. Society of Petroleum Engineers, 1995.
- Cooper, M.P., et al. *Determining the influence of pore-scale geometry on wormhole formation* H21M-1931, AGU Fall Meeting, 2019.
- Izgec, O., D. Zhu, and A. D. Hill. "Numerical and experimental investigation of acid wormholing during acidization of vuggy carbonate rocks." *Journal of Petroleum Science and Engineering* 74.1-2 (2010): 51-66.
- Conference Presentations from PIN43 and PIN44**
- Szymczak, P., et al. *Combined neutron and X-ray time-resolved tomography of wormhole growth in dissolving limestones*. 1-17.12.2020. AGU, Fall Meeting, 2020.
- Szymczak, P., et al. *Wormhole Growth in Dissolving Limestones: Insights from 4D Tomography*. EGU21-13883. EGU Meeting, 2021.

#### Working Paper

- Cooper, M.P., et al. "Dynamics of wormhole growth captured by high time resolution tomography." In preparation.



(C) The flow field after an additional 3 hours of dissolution. (D) The wormhole geometry during C. The wormhole geometry in D closely tracks the experimental flow field in A. A branch not indicated in the flow field of A formed, however it is inactive.

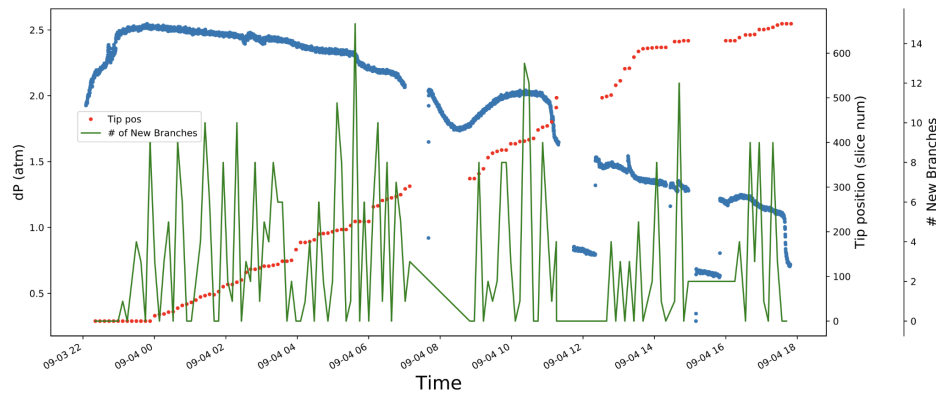


Figure 2. Pressure drop in the sample as a function of time (blue points) correlated with the wormhole tip position and number of new branches extracted from the tomographic images. Large peaks in new branches precede tip jumps and pressure drops, indicating this

parameter may predict jump/drops and thus act as a probe for rock properties.



Figure 3. The final wormhole from conical experiment PIN44.

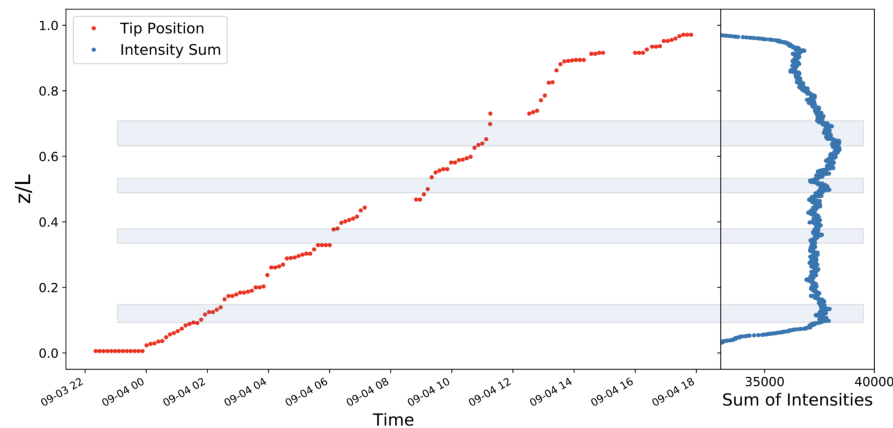


Figure 4. Mean grayscale intensity of all of the pixels in a cross-section perpendicular to the core axis versus tip position evolution. Local large intensity peaks are interpreted to correspond to higher grain fraction within the rock by CT theory and thin sections of Pinchow limestone.. Correlation between intensity peaks and tip position indicate the

wormhole velocity increases when entering lower permeability regions, perhaps due to less available paths increasing the local fluid velocity.